Structural integrity test of prestressed concrete containment vessel for Tsuruga Unit No. 2 Nuclear Power Station

S.Tamura
The Japan Atomic Power Co., Construction Department, Tokyo, Japan
K.Nagata
Mitsubishi Heavy Industries Ltd, Steel Structure Department, Kobe-shi, Japan
T.Takeda, T.Yamaguchi & T.Nakayama
Ohbayashi Corporation, Technical Research Institute, Tokyo, Japan

1 INTRODUCTION

Tsuruga Unit No. 2 Nuclear Power Station of The Japan Atomic Power Company (Pressurized Water Reactor, 1160 Mwe), which is the first in Japan where a Prestressed Concrete Containment Vessel (PCCV) was adopted, has been completed. A PCCV is an important structure requiring aseismic safety, leak tightness, radiation shielding capability and pressure resistance. Therefore, a high degree of safety of the PCCV must be secured. Accordingly, in introducing the PCCV to Japan, various verification tests were carried out to understand the structural performance of the PCCV and confirm the reliability of its design (ref. 1,2). In addition to those tests, a Structural Integrity Test (SIT) was conducted in Feb. 1986 as a final acceptance test of the PCCV of Tsuruga Unit No. 2.

This report discusses the results of the SIT on the PCCV. The test was carried out simultaneously with an Integrated Leak Rate Test (ILRT) under the same pressure sequence.

2 OUTLINE OF PCCV OF TSURUGA UNIT NO. 2

The outline of the PCCV of Tsuruga Unit No. 2 is shown in Fig. 1. The PCCV is covered by the Reactor External Building and is composed of a hemispherical top dome (inside diameter: 43.0 m, wall thickness: 1.1 m) a cylindrical shell (inside diameter: 43.0 m, height: 43.0 m, wall thickness: 1.3 m) of prestressed concrete and a base mat (thickness: 8.0 m) of reinforced concrete. A steel liner is provided at the inside surface of the PCCV to assure leak tightness. The base mat has a tendon gallery, while the cylindrical shell and hemispherical top dome have three buttresses. As shown in Fig. 2, vertical-direction prestress was introduced by inverted U tendons arranged in two orthogonal directions at the dome area, and circumferential-direction prestress by hoop tendons of lengths corresponding to the central angle of 240 deg along the wall in the BBRV post-tensioning systems using tendons of 1000-ton capacity. The prestressing load was set so that the effective prestressing force, considering reductions due to creep and drying shrinkage of concrete, relaxation of prestressing steel, etc. during the 40-years service life of the plant, would be a quantity corresponding to external pressure more than the sum of 1.2 times the design internal pressure and the membrane force due to earthquake load. The design internal pressures and prestressing forces on the PCCV are shown in Table 1.

3 TEST PROCEDURE

3.1 Pressurization of the Containment Vessel

The test was performed according to the pressure sequence shown in Fig. 3. The pressurization rate was 0.1 kgf/cm^2G per hour, and the maximum test pressure of 4.5 kgf/cm^2G (1.125 times the design pressure) was reached roughly 3 days later. The depressurization rate was 0.2 kgf/cm^2G per hour.

3.2 Measurements

As this was the first SIT to be carried out in Japan, multifarious measurements of displacement, strain, tendon force, temperature and inspections of cracking at the concrete surface were made.

Displacements were measured for 51 points including: radial and vertical displacements of the dome and cylindrical shell, and longitudinal and transverse diameter changes of the Equipment Hatch (E/H opening). Representative examples of displacement measurement locations are shown in Fig. 4. Weights were attached to the ends of invar wires stretched across the measurement sections to apply constant tensile forces and the movements of the invar wire ends were measured by linear variable displacement transducers. Strain measurements were made with electrical resistance strain gages, tendon force measurements by load cells, and temperature measurements by thermocouples, respectively. Concrete surface crack inspections were carried out on zones demarcated at the 8 places of cylindrical shell: portions at mid-height of the wall, intersecting portion of cylindrical shell and buttress, intersecting portion of cylindrical shell and dome, periphery of E/H, peripheries of air locks (2 locations), and the portion where small openings were concentrated.

3.3 Temperature Variation Through The Test

The representative time-dependent changes in temperature during testing are shown in Fig. 3. The internal air and PCCV wall temperature remained more or less constant during pressurization, but the temperature declined gradually during depressurization. Parenthetically, from the start of pressurization, the variation in the internal air temperature was -1.2°C at the maximum pressure, and -7.0°C at the time of completion of depressurization. With such variation in the internal air temperature, the average temperature variation in the wall mid-height of the cylindrical shell was -0.1°C when the maximum pressure was reached, and -1.2°C when depressurization was completed. Similarly, the overall average temperature variations in the PCCV wall were -0.2°C and -2.1°C at the maximum pressure and completion of depressurization, respectively. It was understood that the temperature variation was small because pressurizing air was chilled by air cooler to remove humidity contained in the air.

4 SIMULATION ANALYSIS

4.1 Analytical Method

In order to simulate behaviors during pressurization, the design value was corrected using the equivalent Young's modulus which considered the contributions to stiffness of reinforcing bars, prestressing tendons, steel liner, and the Young's modulus of concrete test pieces at the time of the SIT. The design analysis was based on three-dimensional FEM elastic analysis ignoring steel members.

4.2 Evaluation of Measured Values

The displacement measurements were corrected evaluating thermal expansions of invar wires due to the internal air temperature variations and the thermal expansion of the PCCV due to temperature variation.

5 TEST RESULTS AND DISCUSSIONS

5.1 Displacements

Representative examples of internal pressure-displacement relationships are shown in Fig. 5. The internal pressure-displacement relationships indicate roughly elastic behaviors coinciding well with the calculated values. The ratios of the measured displacement values to the calculated values at the maximum pressure were 1.04 for [10B-DV], 0.79 for [4K-DH], and 1.05 for [3-2L3-DH]. The average ratio of radial displacements at 10 points at wall mid-height was 0.84. The ratios of the measured residual displacement values when 24 hours had elapsed after complete depressurization to displacement at the maximum pressure were 9% for [10B-DV], 10% for [4K-DH], and 8% for [3-2L3-DH]. Roughly 90% or more recovery of displacement was recognized.

Fig. 8 shows the displacement distributions at the maximum pressure for the vertical cross section containing the E/H (Cross section L) and the horizontal cross section at the wall mid-height (Cross section 4). Excluding those in the buttresses, the measured and calculated values coincided fairly well.

5.2 Reinforcing Bar Strains

Representative examples of pressure-membrane strain relationships are shown in Fig. 7. The figure for the dome apex (Cross section 10) is the average value for two directions, and those at the wall mid-height (Cross section 4) are the average value for 8 locations not including the E/H and buttresses. The elastic behavior of the PCCV could be seen from the results of strain measurements. These strain measurements coincided with the calculated values. At the maximum pressure, the ratios of measured values to calculated values were 1.12 times at the dome apex, 1.05 times for longitudinal direction and 1.11 times for circumferential direction at the wall mid-height. The membrane strain distributions at Cross section L and Cross section 4 at the maximum pressure are shown in Fig. 8. The measured values corresponded well with the calculated value not only at areas of constant wall thickness and non-openings, but also at the E/H and buttresses.

The displacements determined from membrane strains and measured displacement values are compared in Table 2. The membrane strain given in the table is the average value. As shown in the table, displacements calculated from membrane strains are 0.88 to 1.40 (average 1.04) times the measured displacement value, and the conformity between the two can be seen.

5.3 Tendon Force Variation

As shown in Fig. 9, the relationship between pressure and tendon force is roughly linear. The amounts of variation in force at the maximum pressure were 13.9 and 15.2 tons at opposite ends of the hoop tendon, and 3.8 and 6.3 tons at opposite ends of inverted U tendons. The amount of variation was approximately 2% for hoop tendons in relation to tendon force just before start of pressurizing. Those measured forces were small in comparison with the values obtained assuming elongation of the PCCV and that of tendon to be equal (20.4 tons for hoop tendon, 13.2 tons for inverted U tendon).

5.4 Inspection of Concrete Surface

A representative example of recording of cracks having widths of 0.2 mm and larger is given in Fig. 10. As shown in this figure, the cracks observed were limited as to both length and width. These are fine cracks due to shrinkage of concrete that were widened during pressurization. The cracks were more or less the same at other inspection zones also, and new structural cracks due to pressure were not seen. The amount of variation in crack width from the start of pressurization to the maximum pressure was not more than approximately 0.2 mm.

6 CONCLUSIONS

The following conclusions were drawn as a result of Structural Integrity Tests of the PCCV for Tsuruga Unit No. 2 Nuclear Power Station.

1) Pressure-displacement relationships and pressure-strain relationships were more or less linear.
2) The measured displacement values at the maximum pressure (4.5 kgf/cm^2 G) corresponded well with calculated values. Correspondence with converted displacement obtained from strain and measured displacement was also good.
3) The residual displacement when 24 hours had elapsed after completion of depressurization was not more than 10% of the displacement at the maximum pressure.
4) The variation in tendon force at the maximum pressure is smaller than the calculated value in proportion to the elongation of the PCCV.
5) Although fine surface cracks due to shrinkage of concrete were seen, new structural cracks due to pressure were not observed.

Further, in the ILRT carried out at the same time, the leakage rate of the PCCV was evaluated at 0.016% of volume per day. It is much smaller than the design value of 0.1% of volume per day. Accordingly, it was confirmed that the PCCV not only possessed pressure resistance and leak tightness, but also structural properties that coincided sufficiently well with calculated values. Consequently, structural performance of the Tsuruga Unit No. 2 Nuclear Power Station was assured.

REFERENCES

(1) Kato, M., Tamura, S., Watanabe, Y., Takeda, T., Nakayama, T., and Omote, Y., "Dynamic and Static Loading Tests on 1/30 Scale Model of Prestressed Concrete Containment Vessel," Paper K14/10, SMiRT 6, Paris, 1981

(2) Ogaki, Y., Kobayashi, M., Takeda, T., Yamaguchi, T., and Yoshioka, K., "Horizontal Loading Tests on Large-Scale Model of Prestressed Concrete Containment Vessel," Paper J4/2, SMiRT 6, Paris, 1981

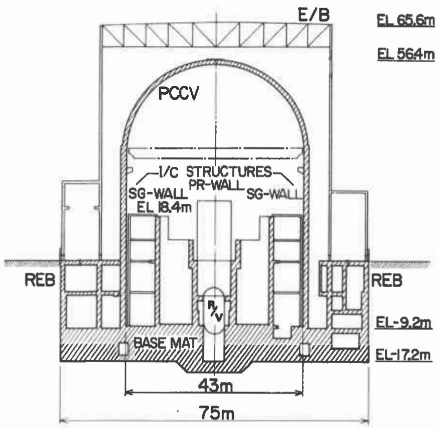

Fig. 1 Outline of Tsuruga Unit No.2 Nuclear Power Statio..

Table 1 Design Pressure and Prestressing Forces

Item		Stress **
Design Pressure (4.0 kgf/cm^2 G)	vertical	31.6 kgf/cm^2
	hoop	66.1 kgf/cm^2
Prestress *	vertical	52.3 kgf/cm^2
	hoop	84.6 kgf/cm^2

* Applied effective prestress after 40 years plant life
** Membrane stress of shell

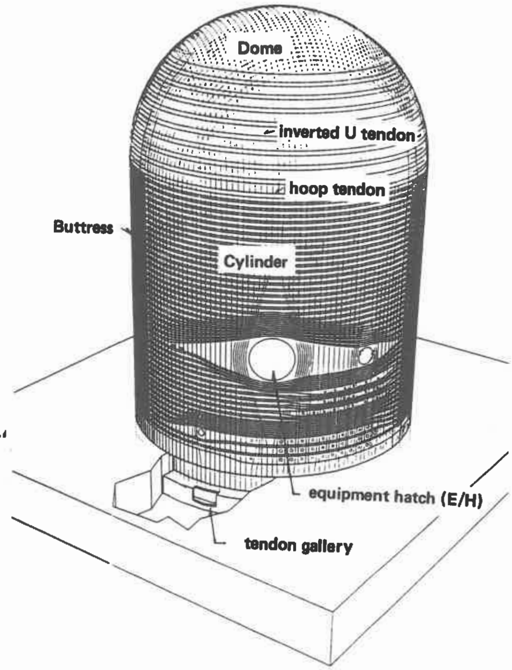

Fig. 2 Tendon Arrangement

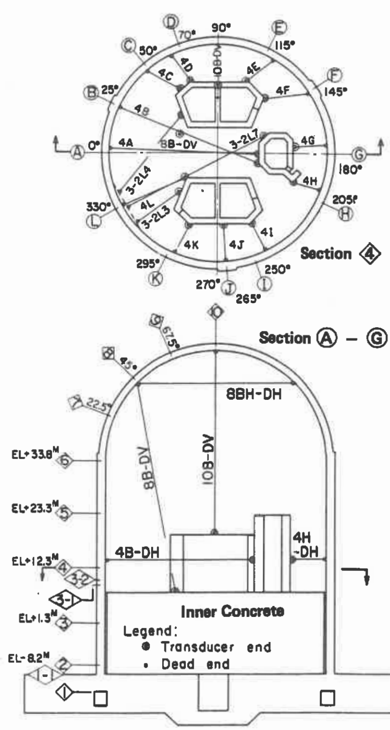

Fig. 4 Invar Wire Locations

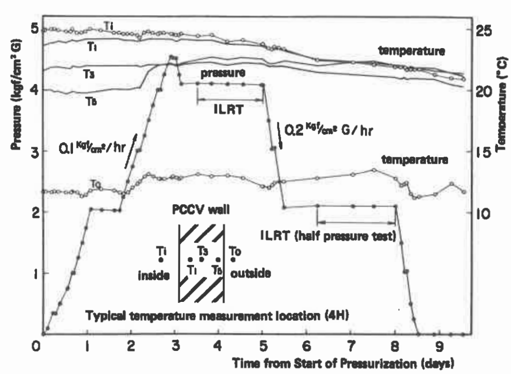

Fig. 3 Pressure/Temperature Time History

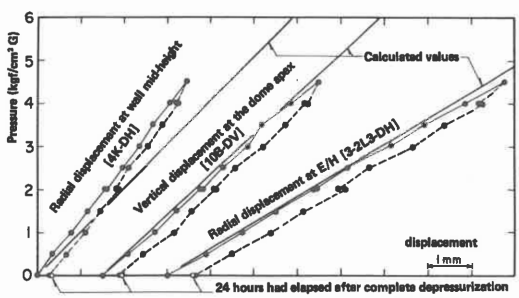

Fig. 5 Pressure-Displacement Relationships

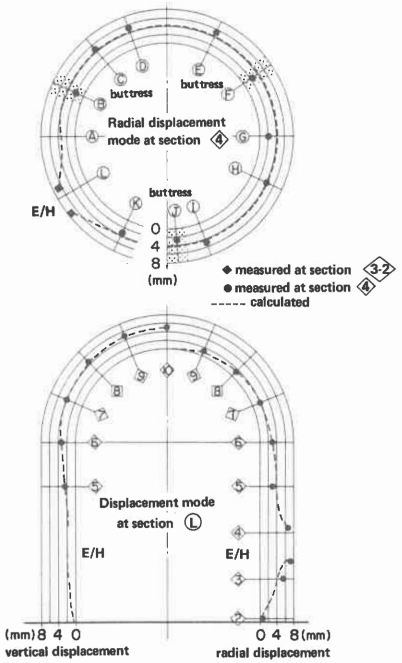

Fig. 6 Displacement Distribution at The Max Pressure

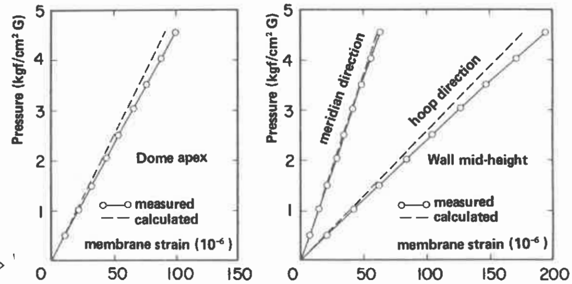

Fig. 7 Pressure-Membrane Strain Relationships

Table 2 Comparison of the Displacements Determined from Membrane Strain with Measured Displacements

Section	vertical displacement				radial displacement			
	membrane strain		disp*	②/③	membrane strain		disp*	⑤/⑥
	① *1 $\varepsilon_\phi(10^{-6})$	② *2 δv(mm)	③ δv(mm)		④ *1 $\varepsilon_\theta(10^{-6})$	⑤ δr(mm)	⑥ δr(mm)	
⑩	100	5.62	5.00	1.12				
⑨	83	5.46	5.45	1.00	122	1.03	1.05	0.98
⑧	110	4.99	4.81	1.04	111	1.73	1.27	1.36
⑦	92	4.30	3.92	1.10	101	2.06	2.03	1.01
⑥	99	3.48	3.56	0.98	137	3.03	3.29	0.92
⑤	78	2.78	2.59	1.07	175	3.88	3.25	1.19
④	63				194	4.30	3.73	1.15
③	70				164	3.63	3.89	0.93
②	55				19	0.42	0.49	0.86

*1 average values excluding those in the portion where wall thickness vary

*2 The vertical displacements of the base mat (0.8 mm at the test presure) were added

* measured displacement

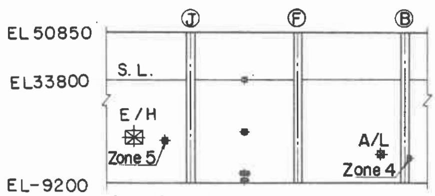

Location of crack inspection areas

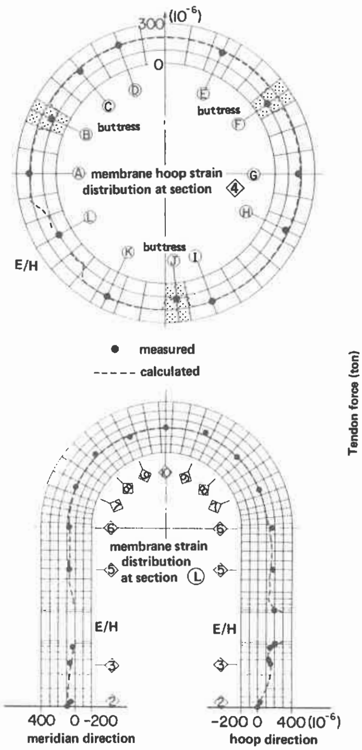

Fig. 8 Membrane Strain Distributions at the Max Pressure

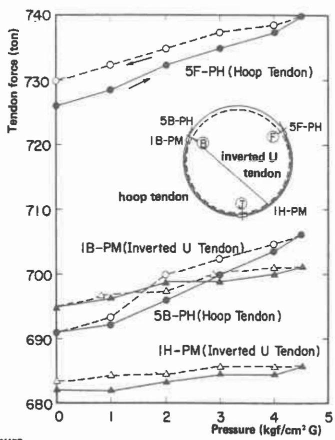

Fig. 9 Pressure-Tendon Force Relationship

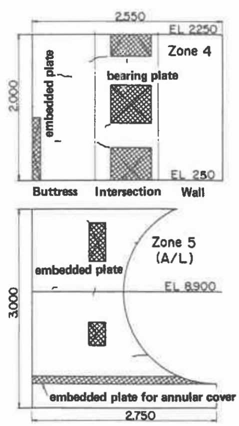

Fig. 10 Concrete Surface Crack Patterns